Fiber Matrix Model of Sclera and Corneal Stroma for Drug Delivery to the Eye

Aurélie Edwards
Dept. of Chemical Engineering, Pennsylvania State University, University Park, PA 16802

Mark R. Prausnitz
School of Chemical Engineering, Georgia Institute of Technology, Atlanta, GA 30332

A model derived from fiber matrix theory to predict the permeability of the eye's fibrous tissues, namely the sclera and corneal stroma, to water and solutes ranging from low molecular-weight drugs to macromolecules was developed. The model is based upon the ultrastructure of the cornea and the sclera; all parameters correspond to the geometrical and physicochemical characteristics of the eye and solutes, and are estimated from independent literature data. Comparison of our predictions with a large set of experimental data shows good agreement. The model suggests that important factors controlling diffusion rates across the sclera and stroma are tissue hydration, tissue thickness, and the size and volume fraction of proteoglycans present in these tissues. Applications to ocular drug delivery and treatment of glaucoma are discussed.

Introduction

One of the greatest challenges in drug delivery is the targeted administration of drugs to precise locations in the body (Robinson and Lee, 1988; Hsieh, 1994). Drug delivery targeted to the eye is especially difficult due to low ocular tissue permeability and convection of drugs to other locations (Lang, 1995; Tasman, 1995). Delivery with topical drops is limited by slow diffusion across the cornea into the eye and unwanted convection and diffusion of tear fluid away from the cornea. Systemic delivery is governed by drug diffusion across blood-vessel walls and through the mostly fibrous tissues of the eye, as well as convective transport in the vessels. Delivery by local injection involves diffusion through internal ocular tissues and, for peribulbar injection, diffusion across the sclera of the eye.

Because many of the challenges associated with ocular drug delivery stem from diffusive and convective transport phenomena that are difficult to control, a model that predicts ocular tissue permeability based only on physicochemical properties and tissue microstructure could help identify the main factors governing transport rates and thus suggest novel means of altering these properties for improved drug delivery. Moreover, a model predicting hydrodynamic permeabilities may suggest new approaches to treat glaucoma, a condition where water flow out of the eye is impeded, thereby increasing the internal pressure of the eye (Tasman, 1995). Unfortunately, no such model currently exists.

Although predicting rates of drug transport across the eye has received some attention in the literature, existing models postulate semiempirical expressions with unknown constants and rely on data fitting to determine the values of needed parameters (Cooper and Kasting, 1987; Grass et al., 1988; Yoshida and Topliss, 1996). In this study, we have developed a predictive model to describe transport across the eye's fibrous, largely acellular tissues: the corneal stroma and the sclera. We have also considered transport across the corneal endothelium by a paracellular route (i.e., between cells). In contrast to previous approaches, all the parameters of our model correspond to geometrical and physicochemical characteristics of the eye and solutes, and were obtained from independent measurements reported in the literature (i.e., they are not fitted). Our model of sclera and stroma can provide direct insight into drug delivery across the sclera, a promising route for local delivery to the retina, and forms the basis for future analysis of transport across the cornea, of which the stroma is an important part. To complete this picture of transport in the eye, future studies will need to address the cellular epithelia: corneal epithelium and conjunctiva.

Correspondence concerning this article should be addressed to A. Edwards.

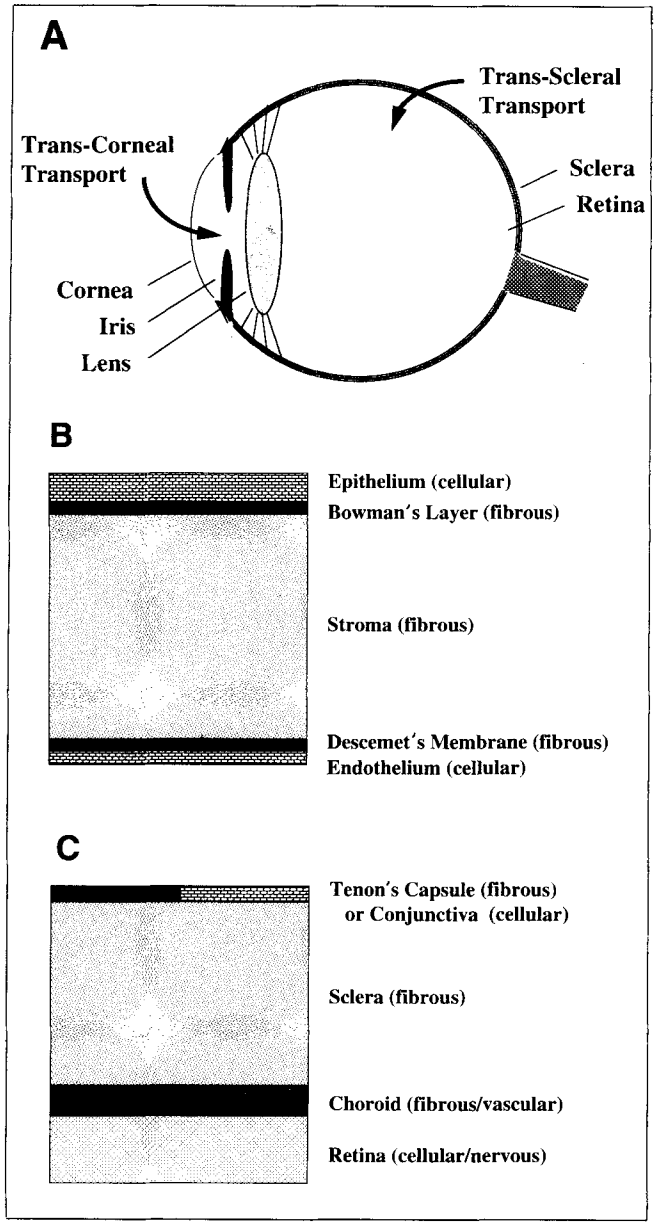

Figure 1. (A) Eye, (B) cornea, and (C) sclera with associated tissues.

Drug delivery to the eye is often by a transcorneal route (e.g., eye drops), or, less frequently, a transscleral route (e.g., peribulbar injection). Drawings are not to scale.

Overview of Ocular Anatomy

The eye can be viewed as a deformed spherical shell of tissue with a diameter of 23–24 mm (Fatt and Weissman, 1992) (Figure 1a). Its interior is filled largely with water, as well as additional structures such as the lens and iris. The transparent portion of this shell is the cornea, which represents 7% of the surface area on a human eye and measures 0.5–0.7 mm in thickness. The sclera is 0.1–1.0 mm thick and covers the remainder of the eye's outer sheath. The frontal portion of the sclera can be seen externally as the "white of the eye."

The cornea is a multilayered tissue containing a superficial layer of epithelial cells, followed deeper by Bowman's layer, stroma, Descemet's membrane, and finally a monolayer of endothelial cells at the base (Figure 1b). The rate-limiting barriers to transcorneal transport are generally the epithelium, endothelium, and stroma.

The sclera is a fibrous connective tissue that gives the eye its shape (Figure 1c). On its anterior surface adjacent to the cornea, the sclera is covered by conjunctiva, a transparent layer of cells. The remainder of the sclera has an outer layer called Tenon's capsule. The sclera is lined internally by the choroid, which contains blood vessels, and the retina, which contains the nerves involved in sight. Transport across this tissue is governed anteriorly by both sclera and conjunctiva, and posteriorly by sclera.

Structural Assumptions

The main constituents of the stroma are water (78% of the total weight at normal hydration), collagen (mostly type I; 15%), glycosaminoglycans (GAGs; 1%), noncollagenous proteins (5%; some of which are bound to the GAGs), and salts (1%) (Fatt and Weissman, 1992). The collagen fibers provide the main structural component of the stroma and are organized in a stack of approximately 200 lamellae, or bundles, which run parallel to the surface and are each about 2 μm thick. Within each lamella, the parallel collagen fibrils form a hexagonal array. The fibers are relatively uniform in diameter (20 to 33 nm), and have a relatively constant center-to-center spacing (60 nm; Fatt and Weissman, 1992). The ground substance (the amorphous, nonoriented gel constituted by the proteoglycans and noncollagenous proteins; see below). The stroma also contains cells called keratocytes, which occupy 3 to 5% of the total volume (Fatt and Weissman, 1992). The presence of these cells was not accounted for in this study, as they do not form a continuous barrier but act primarily as a small excluded volume.

The chemical composition of the sclera is similar to that of the stroma. The sclera's water content ranges between 65 and 75% (Foster and Sainz de la Maza, 1994). Collagen makes up 75% of the dry weight (Foster and Sainz de la Maza, 1994; Fatt and Weissman, 1992), noncollagenous proteins 10%, and GAGs 1% (Fatt and Weissman, 1992). This means that GAGs represent a significantly smaller fraction of the sclera than the stroma. The geometry of collagen fibers in the sclera is also significantly different from the stroma: the diameter of the collagen fibers in the sclera is much more variable, ranging from 30 nm to 300 nm (Fatt and Weissman, 1992); their center-to-center spacing varies between 250 and 280 nm; and while the lamellae run parallel roughly anterior to posterior, they cross each other increasingly as they travel posteriorly. The sclera also contains a small number of isolated fibroblast cells that were not accounted for in our model.

Summarized in Table 1 is the chemical composition of the two membranes expressed on a weight and volume percentage basis under typical experimental conditions. When the corneal epithelium is removed, the corneal thickness increases by 0.2 mm in rabbits due to swelling caused by increased water uptake (Edelhauser et al., 1982). Interpolating the data of Fatt and Weissman (1992) for corneal thickness as a function of hydration, we estimated that the stromal hydration is then 86%. The hydration of sclera was taken as 70%.

Table 1 Chemical Composition of the Corneal Stroma and Sclera

Constituent	Stroma*	Sclera	Stroma	Sclera
Water	86.0 wt. %	70.0 wt. %	89.7 vol. %	77.7 vol. %
Salts	0.64 wt. %	4.2 wt. %	0.19 vol. %	1.3 vol. %
Collagen	9.6 wt. %	22.5 wt. %	7.3 vol. %	18.4 vol. %
GAGs	0.63 wt. %	0.3 wt. %	0.45 vol. %	0.23 vol. %
Noncollagenous proteins:	3.2 wt. %	3 wt %		
GAG-associated			0.68 vol. %	0.68/0.34vol. % **
Free			1.7 vol. %	1.7/2.1 vol. % **

*The composition of the stroma given in the text corresponds to the normal physiological water content of 78%. This table expresses stroma composition based on the water content of deepithelized stroma (86%) used in experiments.
**The two values correspond to our first and second assumptions, respectively (see text).

Previous analysis (Ethier, 1983) has shown the importance of noncollagenous proteins in determining the permeability properties of the stroma and sclera. Some of these noncollagenous proteins are associated with the GAGs, and together form proteoglycan complexes (the GAGs form side chains that are chemically linked to a core protein). The remaining noncollagenous proteins are referred to as free protein. In stroma, the weight percentage of the GAG-associated proteins (i.e., the core proteins of the proteoglycan complexes) has been estimated as 1.5 times that of the GAGs (Axelsson and Heinegård, 1978; Ethier, 1983). Assuming that all the GAGs are protein-associated, the weight percentage of the GAG-associated protein should be 1.5%. Moreover, since total noncollagenous protein represents 5% of the stroma, the weight percentage of the free protein must be 3.5%.

To the best of our knowledge, no measurements of the GAG-associated protein weight or volume fraction have been reported for the sclera. Two approaches were thus considered. In the first one, we assumed that the mass ratio of GAG-associated to free noncollagenous protein is the same in the stroma and sclera (assumption 1). According to this hypothesis, GAG-associated protein constitutes 0.9% of the total mass in the sclera, and free protein 2.1%. As a second approach, we assumed that the mass ratio of the GAG-associated protein to the GAGs is the same in both the stroma and sclera (assumption 2), yielding a weight percentage in the sclera of 0.45% for GAG-associated protein and 2.55% for free protein. To convert from weight to volume percentage in both sclera and stroma, the following estimates of the specific volume of each constituent were used: 0.73 cm^3/g for collagen (Itoi, 1961); 0.74 for free protein (Lehninger et al., 1993); 0.28 for salts (Weast, 1996); and 0.67 for the proteoglycan constituents (Axelsson and Heinegård, 1978). The latter value corresponds to nonhydrated molecules. The hydrated volume, which accounts for water molecules that are tightly bound to proteoglycans, might be more appropriate for our calculations if diffusing molecules do not have access to the space occupied by the bound water. However, since no literature estimate of the hydrated specific volume of proteoglycans was found, nonhydrated values were employed.

The complex structure of the stroma and sclera was modeled based on the following simplifying hypotheses. As shown in Figure 2, we assumed that the collagen fibrils of the sclera and stroma are arranged in hexagonal arrays of cylinders within each lamella, and that at the larger scale, the lamellae themselves form hexagonal arrays of parallel cylinders of radius 1 μm. While this is approximately correct in the stroma, we have disregarded the fact that there is some interweaving of the lamellae in the sclera. Both the collagen fibrils within the lamellae and the lamellae themselves are surrounded by ground substance, an amorphous, nonoriented gel, constituted by the proteoglycan complexes. The radius of the GAGs was taken as 0.5 nm (Ogston et al., 1973), and that of the associated proteins as 0.35 nm (Ethier, 1983). The collagen fibril diameter was assumed to be constant despite the existing range, and taken as 30 nm in the stroma (the average value reported by Meek and Leonard, 1993) and 133 nm in the sclera (the latter value being chosen by assuming that the collagen volume fraction in the lamellae is the same in the stroma and in the sclera). The center-to-center spacing between the fibrils is 60 nm in the stroma; an average value of 265 nm was chosen for the sclera.

The thickness of the sclera was taken as 0.6 mm in both humans and rabbits (Fatt and Weissman, 1992), and 0.8 mm in cows (Maurice and Polgar, 1977). That of the stroma was taken as 0.45 mm in humans and 0.35 mm in rabbits at normal hydration (78%), and 0.75 mm in humans and 0.55 mm in rabbits under experimental conditions (86% hydration, data interpolated from Fatt and Weissman, 1992).

In most studies reporting permeability data for the stroma, the stroma had been stripped of the epithelial layer above, but the endothelium (as well as Descemet's membrane, and perhaps Bowman's layer and the basement membrane) were left attached. We therefore included the endothelium in our

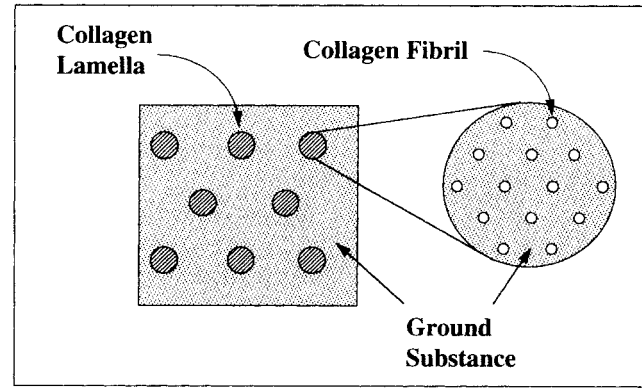

Figure 2. Idealized representation of the microstructure of corneal stroma and sclera.

Both the collagen fibrils within each lamella and the lamellae themselves within the overall layer form hexagonal arrays of cylinders. Both are also surrounded by ground substance.

analysis of transstromal transport and found that the contribution of the endothelial layer to the overall barrier properties is significant. Direct experimental data also indicate that the endothelium can present a significant diffusional resistance (Grass and Robinson, 1988). The endothelial cells are about 20 μm in diameter and 4 to 5 μm thick, and form a mosaic surface in a monolayer. The cells are separated from each other by spaces about 20 nm wide (Fatt and Weissman, 1992), which we modeled as slits between parallel cells. The zonulae occludentes that occasionally join the cells were neglected. All compounds were assumed to diffuse through the intercellular slits and not to penetrate the cells. Transport pathways across the cells were neglected in this study, which should be valid for compounds that are hydrophilic and possibly charged. However, uncharged lipophilic compounds could partition into cell membranes and thereby diffuse across the cells. This issue should be addressed in future studies.

Mathematical Model

The predictive model we developed in this study to determine the water and solute permeability of the stroma and the sclera is based upon recent results from fiber-matrix theory. Modeling the stroma and the sclera as fiber matrices, calculations were performed successively at three different length scales: the microscale of the ground substance, which contains randomly oriented proteoglycans in an aqueous milieu; the mesoscale of each collagen lamella, consisting of a periodic array of collagen fibers surrounded by the ground substance; and the macroscale of the overall membrane in which, the lamellae themselves are arranged in a regular manner within the ground substance.

Hydrodynamic permeability

The flow resistance of a membrane is characterized by its hydrodynamic (or Darcy) permeability $K = \mu v/\nabla p$, where μ and v are the viscosity and velocity of water, respectively, and ∇p is the pressure gradient; K is generally assumed to be constant, independent of the pressure gradient across the membrane. To determine the hydrodynamic permeability of the sclera and stroma, we first considered the microscale conductivity of the ground substance, which we modeled as a fibrous matrix of proteoglycans in saline. In stroma, keratan sulfate (KS) proteoglycans contribute the largest population of glycosaminoglycans (Klintworth, 1982). Based on molecular-weight measurements of the different constituents of KS proteoglycans in cows, Axelsson and Heinegård (1978) estimated that the average KS proteoglycan contains one to three KS chains; similar results were obtained in rhesus monkeys (Hassell et al., 1979). It thus appears reasonable to assume that stromal proteoglycans will not behave as tightly packed monomers (as opposed to cartilage proteoglycans, for instance), but rather as a network of fibers, in which core proteins and GAG side chains form two distinct populations. Following the approach of Ethier (1983), we determined the isotropic Darcy permeability, K_{gs}, of the ground substance as that of a porous medium composed of two different types of randomly oriented fibers, namely, the GAGs and the core proteins:

$$K_{gs} = \left[\frac{n_1}{K_1} + \frac{n_2}{K_2}\right]^{-1} \quad (1 = \text{GAGs}, 2 = \text{core proteins}), \quad (1)$$

where K_i is the Darcy permeability of a porous medium composed solely of fiber type i (present with total volume fraction $\phi_f = \phi_1 + \phi_2$) and n_i, the number fraction of fiber type i in the ground substance, is a function of the volume fractions ϕ_i and the fiber radii r_i (Ethier, 1983):

$$n_i = \frac{\phi_i/r_i^2}{\phi_1/r_1^2 + \phi_2/r_2^2} \qquad i = 1,2. \quad (2)$$

It should be noted that ϕ_i is based upon the volume of the ground substance only, that is, not including the volume occupied by the collagen fibrils.

The individual hydrodynamic permeabilities, K_i, were determined using the results of Jackson and James (1986) for cylindrical rods randomly oriented in all three directions:

$$K_i = \frac{3r_i^2}{20\phi_f}\left[-\ln \phi_f - 0.931 + O(\ln \phi_f)^{-1}\right] \qquad i = 1,2, \quad (3)$$

where terms of order $(\ln \phi_f)^{-1}$ and smaller have been neglected (where necessary, in the remainder, order symbols are explicitly noted). Recent numerical calculations of the permeability of three-dimensional periodic porous media performed by Higdon and Ford (1996) indicate good agreement with the results of Jackson and James (1986). Considering the mesoscale of the lamellae and the macroscale of the overall barrier, the composite hydrodynamic permeability of an array of cylinders was calculated using the results of Perrins et al. (1979) for transport through a spatially periodic medium. Assuming that the flow is orthogonal to the cylinder axis, the ratio, ϵ, of the conductivity of the composite medium to that of the continuous phase (i.e., ground substance) is given by

$$\epsilon = 1 - 2\phi_c\left(T + \phi_c - \frac{C_1\phi_c^6 T}{T^2 - C_2\phi_c^{12}} - \frac{C_3\phi_c^{12}}{T}\right)^{-1} \quad (4)$$

$$T = \frac{1+\alpha}{1-\alpha},$$

where α is the cylinder-to-ground substance conductivity ratio, and ϕ_c is the volume fraction occupied by the cylinders. For hexagonal arrays, the constants are: $C_1 = 0.075422$; $C_2 = 1.060283$; $C_3 = 0.000076$ (Perrins et al., 1979). Equation 4 was used first to determine the mesoscale hydrodynamic conductivity K_{lam} of the lamellar phase (with $\alpha = 0$, since the collagen fibrils are impermeable), and then the macroscale conductivity K of the overall barrier (with $\alpha = K_{lam}/K_{gs}$).

Solute permeability

Stroma and Sclera. The permeability, k_s, of a porous medium to a diffusing solute is related to the effective diffusivity D_{eff} of the medium by

$$k_s = \frac{D_{\text{eff}}}{L} = \frac{\Phi D}{L}, \quad (5)$$

where L is the thickness of the barrier, Φ is the solute partition coefficient (the porous medium-to-free solution concentration ratio at equilibrium), and D is the solute diffusivity in the medium.

We first determined the microscale effective diffusivity of solutes in ground substance. There is at present no rigorous theory for diffusion through a fiber matrix with two types of fiber of comparable size; we therefore considered one population of fibers, with volume fraction $\phi_f = \phi_1 + \phi_2$, and with the radius the number average of the two fiber radii, $r_f = n_1 r_1 + n_2 r_2$. In addition to varying with fiber and solute sizes, the effective diffusivity (ΦD) of a solute in a fiber matrix is expected to depend on charge. A recent study on the effect of electrostatic interactions on diffusion and equilibrium partitioning of proteins in charged gels (Johnson et al., 1995) suggests that ionic strength affects predominantly the partition coefficient Φ, and much less so the diffusion coefficient D. The effects of charge were therefore neglected in calculating D, but were accounted for in determining Φ (see below). Assuming that the hydrodynamic and steric effects that determine the diffusivity can be separated (Clague and Phillips, 1996; Johnson et al., 1996), D was determined as

$$\frac{D}{D_\infty} = F\left(r_s/\sqrt{K_{gs}}\right)S(f) \tag{6}$$

$$f = \phi_f(1 + r_s/r_f)^2, \tag{7}$$

where the factor F accounts for the hydrodynamic interaction between the fibers and the diffusing solutes, and the factor S for steric hindrance. The solute diffusivity in dilute bulk solution is D_∞, and f is the adjusted volume fraction of fibers obtained by assuming that a point-size molecule diffuses in an array of fibers with radius $r_s + r_f$, where r_s is the solute radius. The factor F is derived from Brinkman's calculation (1947) of the drag exerted by the fluid on a translating sphere:

$$F\left(r_s/\sqrt{K_{gs}}\right) = \frac{1}{1 + r_s/\sqrt{K_{gs}} + \frac{1}{3}\left(r_s/\sqrt{K_{gs}}\right)^2}. \tag{8}$$

The Darcy permeability, K_{gs}, was calculated using Eq. 1; its square root, referred to as the screening length, corresponds to the distance over which the effect of the fibers is felt. Neglected in this effective medium approach are the near-field hydrodynamical effects of the network on the solute.

Steric factor S can be estimated following a number of different approaches. For a random fiber network, such as that formed by proteoglycans in ground substance, we used the empirical fit of Johansson and Löfroth (1993) who performed dynamic simulations of hard sphere diffusion in a random-fiber network neglecting all hydrodynamical interactions:

$$S(f) = \exp(-0.84 f^{1.09}). \tag{9}$$

In the ground substance, the partition coefficient Φ_i of a solute with Stokes–Einstein radius, r_s, was determined using recent calculations of Johnson and Deen (1996). The authors extended the partition theory derived by Ogston (1958) to account for electrostatic interactions between charged spherical molecules and charged, randomly oriented cylindrical fibers. The partition coefficient was calculated accordingly as

$$\Phi = \int_0^\infty \frac{2\phi_f(h + r_f + r_s)}{r_f^2} \exp\left[-\phi_f(h/r_f + r_s/r_f + 1)^2\right] \times \exp[-E(h)]\,dh, \tag{10}$$

where h is the surface-to-surface distance between the sphere and the closest fiber. The Boltzmann factor $\exp[-E(h)]$, which corresponds to the relative probability of the corresponding energy state and depends on the net charge of the solute, was determined using the correlation of Johnson and Deen (1996). The parameters needed to calculate the Boltzmann factor are described in the Appendix. In the absence of electrostatic interactions, Eq. 10 yields the widely used relationship of Ogston (1958), $\Phi = \exp[-\phi_f(1 + r_s/r_f)^2]$.

At the mesoscale and macroscale, effective diffusivities were determined by using the results of Perrins et al. (1979) for the conductivity of a composite medium consisting of a hexagonal array of cylinders embedded in a ground matrix (Eq. 4). In these calculations, α is the cylinder-to-surrounding matrix (ground substance) effective diffusivity ratio, and the solid volume fraction is given by $\phi_c = \phi_{cyl}(1 + r_s/r_{cyl})^2$, where ϕ_{cyl} and r_{cyl} are the appropriate cylinder volume fraction and radius, respectively.

Corneal Endothelium. As indicated earlier, we assumed that the only pathway for diffusion across the endothelial layer of the cornea is through the tight junctions, modeled as parallel channels. Lacking information about the surface charge of corneal endothelial cells, we neglected electrostatic effects in the endothelium, although recent simulations of electrostatic partitioning in slit pores indicate that such effects could be significant, particularly for low solute concentrations (Chun and Phillips, 1997). The effective diffusivity of a solute in a slit channel of half-width, W, was determined based upon the results of Panwar and Anderson (1993):

$$\frac{D_{\text{eff}}^{en}}{D_\infty} = f_a\left[1 + \frac{9}{16}\left(\frac{r_s}{W}\right)\ln\left(\frac{r_s}{W}\right) - 1.19358\left(\frac{r_s}{W}\right) + 0.159317\left(\frac{r_s}{W}\right)^3 + O\left(\frac{r_s}{W}\right)^4\right], \tag{11}$$

where f_a is the fractional area of the intercellular openings on the endothelial surface. Assuming a density of 2,000 cells/mm^2 (Fatt and Weismann, 1992), the length of the boundaries between cells (l_b) is approximately given by $(2{,}000/2)\cdot\pi\cdot(20\,\mu\text{m}) \approx 63$ mm for every mm^2 of endothelial surface, and f_a can be estimated as $2W\cdot l_b = 1.3\times10^{-3}$. The endothelium and the stroma form resistances in series, and the permeability of the combined layers is given by

$$k_s = \left[\frac{1}{k_s^{\text{endothelium}}} + \frac{1}{k_s^{\text{stroma}}}\right]^{-1}. \tag{12}$$

Table 2. Solute Permeability of the Sclera

Solute	r_s nm*	Calc. k_s $\times 10^{-5}$ cm/s	Meas. k_s $\times 10^{-5}$ cm/s**
5-Fluorouracil	0.35	12.4	4.4
Bromacetazolamide	0.43	6.89	2.0
Methazolamide	0.46	6.25	3.0–3.7
Ethoxzolamide	0.46	6.69	2.5–3.8
Pilocarpine	0.46	7.83	1.3–2.0
Benzolamide	0.49	5.19	1.5–2.0
Propranolol	0.50	6.87	5.8
Sucrose	0.50	5.80	2.2–4.2
Penicillin G	0.51	4.92	0.8–0.9
Nadolol	0.53	5.99	3.9
Penbutolol	0.53	5.86	7.1
Hydrocortisone	0.54	4.94	0.6–1.2
Timolol	0.55	5.42	4.1
Dexamethasone	0.55	4.77	2.4
Methotrexate	0.58	3.52	2.3
Inulin	1.40	9.47×10^{-1}	$1.7–9.1\times10^{-1}$
Hemoglobin	3.13	$2.99–3.52\times10^{-2}$†	$1.9–7.9\times10^{-2}$
RISA††	3.50	1.53×10^{-2}	$1.0–2.5\times10^{-2}$

*Small solute radii were determined as described in the text. Reported literature values were used for inulin (Liaw and Robinson, 1993), RISA (Johnson et al., 1995), and hemoglobin (Laurent and Killander, 1964).
**Experimental data were reviewed by Prausnitz and Noonan (1997), and adjusted to human tissue thickness (see text).
†The first and second values correspond to molecular charge numbers of −20 and −10, respectively (see the Appendix).
††Radioactive iodinated serum albumin.

Derivation of solute radius

The diffusivity of small compounds was estimated using the Wilke–Chang correlation (Reid et al., 1987). This correlation is based upon the volume at the normal boiling point (V_b), which was determined using the LeBas group-contribution method (Reid et al., 1987). Solute radii were also estimated based on the boiling point volume, assuming that the compounds are perfect spheres. Diffusivities and/or radii of macromolecules were obtained from the literature and related through the Stokes–Einstein equation. Results are summarized in Tables 2–5. Solute diffusivities are inversely proportional to $V_b^{0.6}$ (i.e., to $r_s^{1.8}$) according to the Wilke–Chang correlation for small compounds, and inversely proportional to r_s using the Stokes–Einstein equation for macromolecules. Predicted permeability curves will thus be discontinuous between small solutes and macromolecules (see Figures 4 and 5).

Table 3. Solute Permeability of the Corneal Stroma-Plus-Endothelium to Hydrophilic Compounds

Solute	r_s nm*	Calc. k_s $\times 10^{-5}$ cm/s	Meas. k_s $\times 10^{-5}$ cm/s**
Methazolamide derivative I†	0.41	1.82	1.3
Phenylephrine	0.42	1.83	1.6
Acetazolamide	0.43	1.70	0.8
Bromacetazolamide	0.43	1.72	0.7–1.6
Methazolamide	0.46	1.47	1.4–2.2
Trifluoromethazolamide	0.46	1.48	1.4
Trichloromethazolamide	0.46	1.48	2.9–3.0
Idoxuridine	0.46	1.48	1.3
Trifluorothymidine	0.46	1.42	1.5
Acetazolamide derivative I†	0.47	1.41	0.8
Acetazolamide derivative II†	0.47	1.42	0.7
Benzolamide	0.49	1.32	0.8–1.1

*Solule radii were determined as described in the text.
**Experimental data were reviewed by Prausnitz and Noonan (1997), and adjusted to human tissue thickness (see text).
†Methazolamide derivative I: 5-imino-4-methyl-1, 3, 4 thiadiazoline-2-sulfonamide; acetazolamide derivative I: 2-isopentenyl-amino-1, 3, 4-thiadiazole-5-sulfonamide; acetazolamide derivative II: 2-benzoylamino-1, 3, 4-thiadiazole-5-sulfonamide.

Table 4. Solute Permeability of the Corneal Stroma-Plus-Endothelium to Lipophilic Compounds* (Partial Estimates)**

Solute	r_s nm†	Calc. k_s $\times 10^{-5}$ cm/s	Meas. k_s $\times 10^{-5}$ cm/s‡
SKF 86 607	0.42	1.81	4.2
SKF 86 466	0.44	1.65	4.1
SKF 72 223	0.45	1.61	3.0
Chlorzolamide	0.46	1.51	2.8
Ethoxzolamide	0.46	1.45	3.0 – 3.6
Clonidine	0.47	1.49	3.7
Rauwolfine	0.52	1.22	1.8
Yohimbine	0.57	1.00	2.9
Alpha-yohimbine	0.57	1.00	3.0
Corynanthine	0.57	1.01	2.4

*Lipophilic compounds are classified as such if their octanol–water partition coefficient is much greater than unity.
**Since the model does not account for partitioning into and diffusing across endothelial cells, the theory is not strictly applicable to lipophilic compounds and is expected to underestimate their pemeability (see text).
†Solute radii were determined as described in the text.
‡Experimental data were reviewed by Prausnitz and Noonan (1997), and adjusted to human tissue thickness (see text).

Results and Discussion

To predict the permeabilities of tissues in the eye, we have developed a model derived from fiber matrix theory which uses independently measured values for the geometrical and physicochemical characteristics of the eye and solutes, and which requires no adjustable parameters. We have predicted the permeability of the principal fibrous tissues of the eye (i.e., the corneal stroma and sclera) to water and to solutes

Table 5. Solute Permeability of Stroma

Permeability	r_s nm*	Calc. k_s $\times 10^{-5}$ cm/s	Meas. k_s $\times 10^{-5}$ cm/s**
Phenylephrine	0.42	10.0	4.5
SKF 86 607	0.42	9.75	4.1
SKF 86 466	0.44	8.43	4.4
SKF 72 223	0.45	8.41	3.3
Clonidine	0.47	7.49	3.8
Rauwolfine	0.52	6.04	2.8
Yohimbine	0.57	4.70	3.0
Alpha-yohimbine	0.57	4.60	2.9
Corynanthine	0.57	4.73	2.5
Diffusivity†		Calc. D(cm^2/s)	Meas. D (cm^2/s)**
Hemoglobin	3.13	1.73×10^{-7}	1.02×10^{-7}
BSA	3.50	1.14×10^{-7}	1.1×10^{-7}
IgG	5.00	1.92×10^{-8}	2.3×10^{-8}

*Small solute radii were determined as described in the text. Reported literature values were used for BSA (Johnson et al., 1995) and hemoglobin (Laurent and Killander, 1964). The molecular radius of IgG was calculated from its diffusivity in water (Fatt and Weissman, 1992).
**Experimental data were reviewed by Prausnitz and Noonan (1997), and adjusted to human tissue thickness.
†Experimental values for macromolecules in stroma were reported as diffusion coefficients instead of permeabilities.

ranging from low molecular-weight drugs to macromolecules. Comparison of these predictions with experimental data shows good agreement, as described below.

Hydrodynamic permeability

Using the model described earlier, we predicted the hydrodynamic (Darcy) permeability of corneal stroma and sclera as a function of tissue hydration (H). Theoretical results were compared to the experimental data of Fatt and Hedbys (1970a, b) and are shown in Figure 3 in the form of the least-square fit the authors obtained. As illustrated by the 95% confidence interval limits determined by the authors, experimental variations in the data are significant.

Both in stroma and sclera, our model predicts hydraulic permeability well at large H, but appears to overpredict K as tissue hydration decreases. In stroma, the calculated perme ability remains within the bounds of the 95% confidence interval for H greater than 82%. Under normal physiological conditions (78% hydration), our predicted value of 2.2 nm^2 is just 30% greater than the upper confidence limit, but a factor of 4 greater than the average experimental value (Figure 3a). When the corneal epithelium is removed, as in solute permeability experiments, $H = 86\%$, and the predicted permeability is 4.9 nm^2, which is within the confidence interval and about 2.5 times the least-square fit value (Figure 3a).

In sclera, using our first assumption about the fraction of GAG-associated proteins (as discussed earlier), model estimates of the hydrodynamic permeability remain within the bounds of the 95% confidence interval almost throughout the range of H and are most accurate when H is high. In physiogically hydrated sclera (68% hydration), we obtained a value of 3.6 nm^2 with our first hypothesis, that is, within the confidence interval and about 2.5 times the average experimental value of 1.34 nm^2 (Fatt and Hedbys, 1970b) (Figure 3b). Our second hypothesis yielded a value of 6.9 nm^2, and although assumption 1 also yields permeability values that are too high, the predictions using assumption 1 are consistently closer to experimental values than assumption 2; unless otherwise stated, we shall thus only discuss results based upon our first assumption in the remainder of this section. Under the conditions of typical solute permeability experiments, the hydration of sclera is higher, at 70%, and the predicted Darcy permeability is 4.1 nm^2.

Although the agreement in sclera and stroma is reasonably good, the reason for consistent overpredictions by our model is not clear. There appears to be inherently a lot of scatter when permeability data are plotted vs. volume fraction for a wide range of membranes; as illustrated in the study of Jackson and James (1986), there can be as much as a factor of 4 difference between predicted values of the hydrodynamic permeability (Eq. 3 of this article) and measured values. The discrepancy may also be due to the fact that we underestimated the volume fraction of the proteoglycans by not taking into consideration the shell of tightly bound water molecules (as mentioned earlier). We also neglected the presence of cells in the tissues, keratocytes in stroma, and fibroblasts in sclera. However, this discrepancy cannot be ascribed to the idealization of the collagen lamellae in our model as rods with a uniform radius. Although in reality their diameter varies over a wide range, varying the rod radius does not affect water permeability results, since the overall fraction of collagen in the tissue is known and fixed. Despite some limitations, the predicted water permeabilities represent a significant improvement over previous calculations (Ethier, 1983), which yielded a factor of 6 discrepancy in sclera at normal hydration. This improvement comes from our specifically accounting for the resistance of the collagen lamellae, neglected in the older analysis.

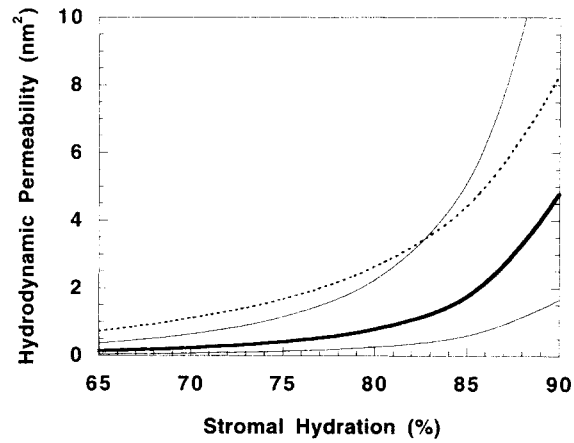

Figure 3a. Hydrodynamic permeability as a function of tissue hydration: stroma.

Thick curve (——) represents the least-square fit to human stroma data of Fatt and Weissman (1992), with the 95% confidence interval limits (——); thick dotted curve (· · ·) represents our theoretical predictions.

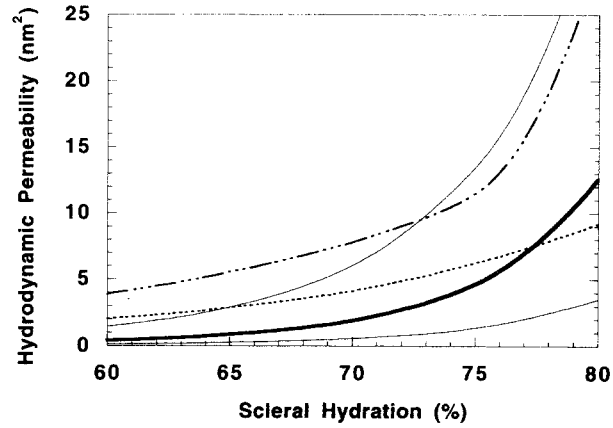

Figure 3b. Hydrodynamic permeability as a function of tissue hydration: sclera.

Thick curve (——) corresponds to the least-square fit to human and rabbit sclera data of Fatt and Weissman (1992), with 95% confidence interval limits (——). Predictions of the model are given for assumption 1 (– – –) and assumption 2 (— · · · —).

Solute Permeability

Predictions of sclera and stroma permeability were obtained as a function of solute radius and charge, as shown in Figures 4 and 5. Solute permeabilities decrease with increasing molecular radius, as expected for diffusion through a ma-

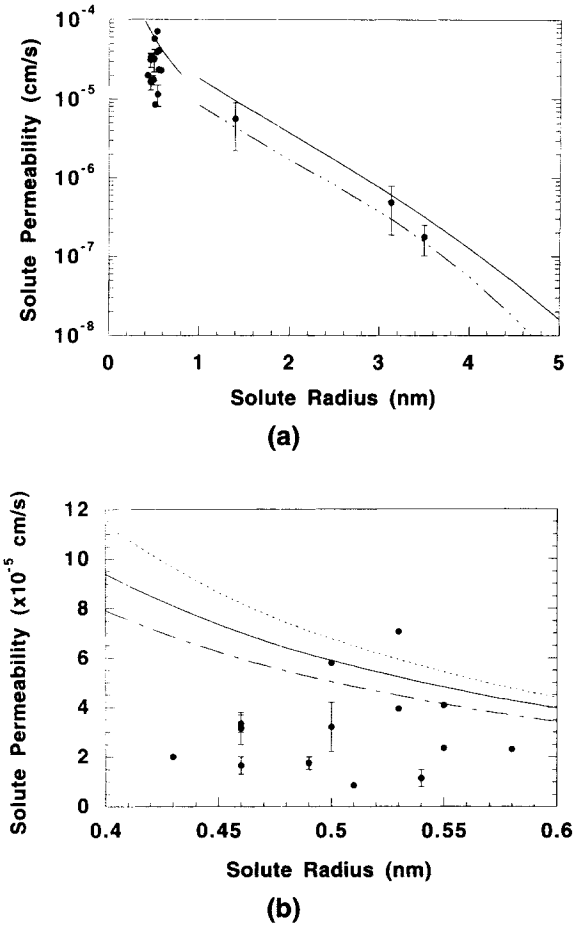

Figure 4. Solute permeability of the sclera as a function of solute radius and charge: (A) for all sizes; (B), for small compounds only.

The filled circles represent experimental data from the literature (reviewed by Prausnitz and Noonan, 1997). Standard deviation bars are shown. Curves correspond to the predictions of our model assuming different solute charge: uncharged (——), +1 charge (– – –), −1 charge (—–—), −20 charge (— · · · —). The break in the curve corresponding to neutral solutes is due to the fact that small solute bulk diffusivities shows a different dependence on molecular radius than macromolecule diffusivities do. Predicted permeabilities generally fall within the range of experimental values. However, those of the smallest compounds ($r_s < 0.5$ nm) are overpredicted. The volume fraction occupied by the GAG-associated protein was taken as 0.68%. In ground substance, the partition coefficient was determined as described in the Appendix; the diffusion coefficient was calculated using Eqs. 6–9, with $K_{gs} = 4.1$ nm^2; $r_f = n_1 r_1 + n_2 r_2 = 0.37$ nm; and $\phi_f = \phi_1 + \phi_2 = 0.0091/(1 - 0.18) = 0.011$. Mesoscale and macroscale permeabilities were then determined using Eq. 4, with $r_c = 15$ nm and 1 μm, and $\phi_c = 0.23$ and 0.88, respectively.

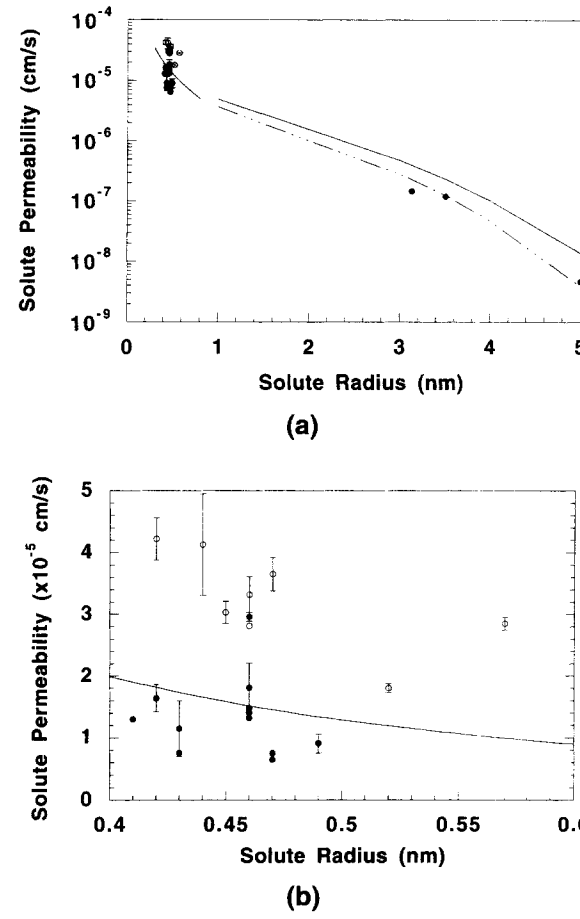

Figure 5. Solute permeability of the corneal stroma-plus-endothelium as a function of solute radius and charge: (A) for all sizes; and (B) small compounds only.

● and ○ represent hydrophilic and hydrophobic compounds, respectively, from experimental data from the literature (reviewed by Prausnitz and Noonan, 1997). Standard deviation bars are shown. Curves correspond to the predictions of our model assuming different solute charge: uncharged (——), −20 charge (— · · · —). Curves corresponding to charges of +1 or −1 are almost superimposed on the uncharged curve and are not shown The break in the curve corresponding to neutral solutes is due to the fact that small solute bulk diffusivities show a different dependence on molecular radius than macromolecule diffusivities do. To convert to permeability values the macromolecule diffusivity data in the literature, we assumed a charge number of −20 for hemoglobin and IgG, and −20.4 for BSA (see Appendix). Predicted permeabilities generally agree with the range of experimental values. As expected, the permeability to hydrophobic compounds is underpredicted. In ground substance, the partition coefficient was determined as described in the Appendix; the diffusion coefficient was calculated using Eqs. 6–9, with $K_{gs} = 4.9$ nm^2; $r_f = 0.39$ nm; and $\phi_f = 0.0113/(1 - 0.07) = 0.0122$. Mesoscale and macroscale permeabilities were then determined using Eq 4, with $r_c = 15$ nm and 1μm, and $\phi_c = 0.23$ and 0.40, respectively. The permeability of the 5-μm-thick endothelium was calculated using Eq. 11 with $W = 10$ nm.

trix with pore sizes of the same order of magnitude as the solutes. Because GAGs impart a negative charge to the stroma and sclera, the permeability to positively charged solutes is greater than that to neutral compounds, which is in turn greater than that to negatively charged solutes.

Theoretical predictions of scleral and stromal permeabilities were compared to experimental data (reviewed by Prausnitz and Noonan, 1997) for over 40 different solutes with radii ranging from 0.35 nm to 5.0 nm (Figures 4 and 5, Tables 2–5). Predicted values generally fall within the range of values reported in experimental studies, demonstrating the ability of the model to predict sclera and stroma permeability for a broad range of compounds. Validation of the model is limited in part by the large variability in the experimental data; this variability is generally inherent to experimental measurements in biological systems. However, our results suggest that

the model adequately describes the most important features that govern transport across these tissues, without a need for adjustable parameters.

Many of the compounds studied experimentally are partially charged at physiological pH. In contrast, theoretical curves are shown in Figures 4 and 5 for only a few integral numbers of charge per molecule. Since the majority of compounds carry a fractional charge, most of the experimental data are not expected to fall exactly on any of the curves, but will lie in between. For solutes with a partial charge, we first used pKa values to determine the fraction of charged molecules, f_c, at the experimental pH, and then calculated the permeability by adding f_c times the permeability of the charged species to $(1 - f_c)$ times that of the uncharged species. Solute permeability values were also calculated on the basis of human tissue thickness data, and experimental results were adjusted accordingly; when the measured data were obtained in different species, they were multiplied by the corresponding species-to-human thickness ratio, thereby correcting the value of L in Eq. 5.

In the sclera, model predictions are only given for our first assumption regarding the volume fraction of GAG-associated proteins (Figure 4, Table 2). As in the case of the hydrodynamic permeability (see earlier), the second hypothesis yielded larger discrepancies between experimental and theoretical results. The predicted permeability to macromolecules is always within the bounds of experimental results. Predictions for many of the small solutes are also within the range of measured values. However, there appear to be some discrepancies, notably for very small ($r_s < 0.5$ nm) negatively charged solutes. It is doubtful that the model underestimates the effects of charge since the permeability to positively charged compounds as well as to negatively charged macromolecules is well predicted. It should also be noted that these discrepancies cannot be due to our underestimating the volume fractions of proteoglycan constituents. Indeed, if we adjust the values of the GAG and associated protein volume fractions in sclera so as to obtain an overall water permeability estimate in agreement with experimental results (see earlier), permeability results change significantly only for macromolecules; the permeability of sclera to a 0.5-nm solute decreases by 10%, that to a 3.0-nm macromolecule by 75%.

The model also predicts the permeability of stroma-plus-endothelium to hydrophilic compounds well (Figure 5, Table 3). As expected, the permeability to lipophilic compounds (Figure 5, Table 4) is underpredicted, since the model does not account for transcellular transport pathways across the endothelium. There is significant scatter in the experimental data for small solutes; permeabilities to compounds of similar size and charge can vary by as much as a factor of 5. This scatter is due in part to the variability inherent to experimental data, but possible differences in solute shape, which the model does not account for, may also explain these discrepancies.

Decoupling the permeability of the stroma from that of the endothelium reveals that for small compounds ($r_s < 1$ nm) both endothelium and stroma are rate-limiting barriers; endothelium permeability is about three to four times smaller than stroma permeability. In contrast, for larger macromolecules the stroma is by far the limiting barrier, its permeability being several orders of magnitude less than that of the endothelium. Solute permeabilities of corneal stroma (without endothelium) are shown in Table 5. The agreement between theoretical and experimental results for macromolecules is very good. Small solute permeabilities appear to be overestimated by the theory by a factor of 2; it should be noted, however, that all the small solute data reported in Table 5 were obtained by Chiang et al. (1986), in whose study we noted some inconsistencies: for some compounds, the permeability of stroma-plus-endothelium was found to be higher than that of stroma only, even when the hydration was lower in the former case. Other reported measurements of stroma-to-endothelium permeability ratios for hydrophilic compounds (Schoenwald, 1985) appear to validate our predictions; for nadolol, for instance, the measured ratio of 4.0 was in excellent agreement with our predicted value, 4.1.

Solute permeability, limitations

This study was motivated in part by the need for new strategies to deliver drugs to the eye. We therefore performed a sensitivity analysis to determine the extent to which permeability is affected by changes in the physiochemical parameters of the model. For drug delivery applications, some approaches to increasing drug permeation into tissues are based on transiently altering tissue barrier properties using physical, chemical, electrical, ultrasonic or other methods (Robinson and Lee, 1988; Hsieh, 1994). Determining the parameters that predominantly control permeability in the eye might lead to novel approaches to increasing tissue permeability for ophthalmic drug delivery.

To identify the principal determinants of water and solute permeabilities within the context of the proposed model, we performed a sensitivity analysis by assessing the effect of a 50% increase in the main parameters. Results are similar for sclera and stroma, and are shown for sclera in Figure 6. Overall, changes in the physicochemical parameters of the stroma and sclera affect the permeability to macromolecules much more than that to smaller compounds. An increase in the volume fraction occupied by the GAGs (or the GAG-associated proteins) reduces water permeability as well as solute permeability due to decreases in the hydrodynamic factor, F, the steric factor, S, and the partition coefficient. Conversely, for a given volume fraction, an increase in GAG or protein radius translates into wider spaces between the fibers, and thus a greater water permeability. In addition, a larger fiber radius corresponds to a smaller adjusted volume fraction f. This in turn leads to increased solute permeabilities due to larger diffusion and partition coefficients. Changes related to GAG-associated proteins result in much more dramatic variations in permeability than similar changes in GAGs, since the former components occupy a larger volume.

The effect of changes in the collagen fibril radius (r_{coll}), for a given collagen volume fraction, are more subtle. When r_{coll} is increased, the fibrils occupy a larger fraction of the lamellae, thereby reducing the mesoscale-to-microscale permeability ratio, but the lamellae then represent a smaller volume fraction of the overall matrix, thus resulting in a higher macroscale-to-mesoscale permeability ratio; as shown in Figure 6, these two effects approximately cancel out.

An increase in tissue hydration significantly increases permeability. (Note that in Figure 6 tissue hydration has only

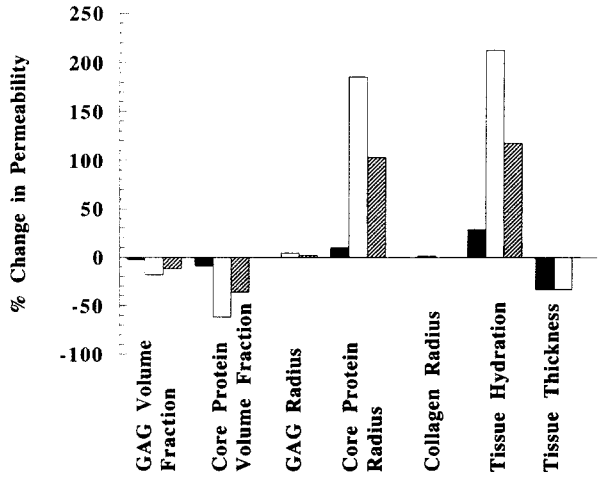

Figure 6. Effect of increases in physicochemical model parameters on water and solute permeabilities for small solutes (black bars), macromolecules (white bars), and water (striped bars).

All parameters were increased by 50%, except for tissue hydration, which was raised from 70 to 80%. Results are given for the sclera, but are representative of the effects in stroma as well. The radii of the small and large solutes were taken as 0.5 and 3.0 nm, respectively, and the solutes were uncharged. Although the permeability to small solutes is relatively unaffected by changes in the model parameters, that to macromolecules is strongly affected by tissue hydration, tissue thickness, and GAG-associated (core) protein fraction and radius.

been increased from 70% to 80%, since a 50% increase is not possible.) This strong dependence on hydration is expected since a greater water content decreases the volume fractions occupied by GAGs and GAG-associated proteins. An increase in tissue thickness proportionately decreases tissue permeability.

We also examined the effects of a 50% increase in the endothelium slit width on corneal stroma-plus-endothelium permeability (data not shown). This change resulted in a 72% increase in the permeability to a small solute of radius 0.5 nm, whereas the permeability to a large solute 3 nm in radius was much less affected (35%). Indeed, as shown before, the rate-limiting barrier for small solutes is largely the endothelium, that for macromolecules is the stroma.

Applications to drug delivery

Changes in the physicochemical parameters of the stroma and sclera have only weak effects on the permeability to small compounds, such as conventional drugs. Indeed, these tissues are already quite permeable to small compounds, which means that transscleral delivery should occur readily, without the need for enhancement. Transcorneal delivery is more difficult, but the rate-limiting barrier is usually not the stroma; transport is mainly limited by the endothelium, the permeability of which can be increased by enlarging intercellular spacing, and by the epithelium, which was not treated in the present analysis.

A more challenging and increasingly important problem is the delivery of macromolecules such as proteins, bioactive carbohydrates, DNA, and other products of biotechnology. Our model suggests that transscleral delivery could be aided by delivering macromolecules across thinner regions of the sclera, as suggested previously by Olsen et al. (1995); human scleral thickness can vary between 0.1 and 1.0 mm at different locations (Tasman, 1995). Additionally, macromolecule transport can be enhanced through increased scleral hydration, which could be achieved by an osmotic, enzymatic, or other mechanism. Transient modification of the architecture of the proteoglycans could also represent a useful approach to improve macromolecule delivery to the eye. This might be achieved via chemical, electrical, ultrasonic, or other approaches. These approaches may also be used to aid transport across the stroma.

There are situations where stroma would be a rate-limiting barrier to macromolecules and enhanced transport would be of interest. For transcorneal transport, the corneal epithelium usually presents a much greater barrier than the stroma. However, if the cornea has been damaged through injury or disease, the stroma could become rate limiting. This could be important if macromolecular drugs are being given topically to treat a corneal injury or disease, and penetration of the drug into the eye is of interest (and may be detrimental). Also, the stroma contains no blood vessels. All communication between the systemic vasculature and cells of the cornea not located at the cornea's outer edge occurs by diffusion through the cornea. For macromolecules, including, for example, those involved in immune response, diffusion through the stroma becomes important.

Glaucoma occurs when the outflow of water from the eye is impeded, often resulting in increased intraocular pressure (Tasman, 1995). Under normal physiological conditions, water leaves the eye largely through a channel near the front of the eye, called the Canal of Schlemm. However, up to 20% of the water drains across the bulk of the sclera (Fat and Weissman, 1992). Therefore, increased hydrodynamic permeability of the sclera could enhance drainage from the eye and thereby aid in treating glaucoma. Methods that increase tissue hydration or create favorable changes in GAG-associated proteins could thus be useful for glaucoma therapy.

Limitations

The proposed model shows good agreement with experimental data and is capable of providing insight into transport phenomena in the eye. Further improvements are limited largely by a lack of experimental data. Notably missing from the literature are experimentally determined values for molecular radii. Because solute permeabilities are predicted as a function of molecular size, the molecular radius of each compound is an essential parameter. Unfortunately, in the majority of cases, we were not able to find the values of r_s in the literature and had to estimate radii using a group-contribution approach, as described earlier. A small change in solute radius has a significant effect on solute permeability, as shown by the slope of the curves on Figures 4 and 5 (doubling the radius from 0.5 nm to 1 nm results in a 4-fold decrease in sclera permeability). Moreover, our assumption that solutes are spherical is another limitation; nonspherical shapes cannot be treated rigorously using our theoretical approach.

Another important yet uncertain parameter in this model is the solid volume fraction occupied by the GAG-associated proteins in the sclera. Two hypotheses were considered in this study; we assumed successively that the GAG-associated protein-to-free protein weight ratio is the same in stroma and sclera, and that the GAG-to-GAG associated protein weight ratio is the same in stroma and in sclera. Since the former assumption yields better estimates of both hydrodynamic and solute permeabilities in the sclera, it appears more reasonable, but experimental measurements will be needed to confirm this hypothesis.

The effects of lipophilicity were neglected in this study, which may limit the applicability of the model for endothelium permeability. As noted earlier, we only accounted for a paracellular transport pathway across the corneal endothelium, whereas small lipophilic solutes are likely to cross this barrier by a transcellular route (partitioning into and diffusing along lipid bilayers). The permeability of stroma-plus-endothelium to lipophilic compounds was thus underestimated, as expected (Table 4). Transcellular transport pathways need to be considered in further studies.

Conclusion

The model presented here is the first to predict the permeability of stroma and sclera to water and solutes without any adjustable parameters. This model is based upon the ultrastructure of the cornea and the sclera; all parameters correspond to the geometrical and physicochemical characteristics of the eye and solutes, and are estimated from independent literature data. Given that there are no adjustable parameters in the calculations, the agreement between the data and the predictions is remarkably good.

Acknowledgments

This work was supported by NSF Grant BES-9707512 (A.E.) and NSF CAREER BES-9624832 (M.R.P.). We thank Jeremy Noonan for his help in acquiring experimental data from the literature, and Drs. Henry Edelhauser and Dayle Geroski for helpful discussions.

Literature Cited

Alcon Surgical. "BSS Plus"(Package Insert), Forth Worth, TX (1991).

Axelsson, I., and D. Heinegård, "Characterization of the Keratan Sulphate Proteoglycans from Bovine Corneal Stroma," *Biochem. J.* **169**, 517 (1978).

Brinkman, H. C., "A Calculation of the Viscous Force Exerted by a Flowing Fluid on a Dense Swarm of Particles," *Appl. Sci. Res.*, **A1** 27 (1947).

Chiang, C.-H., H.-S. Huang, and R. D. Schoenwald, "Corneal Permeability of Adrenergic Agents Potentially Useful in Glaucoma," *J. Taiwan Pharm. Assoc.*, **38**, 67 (1986).

Chun, M.-S. and R. J. Phillips, "Electrostatic Partitioning in Slit Pore by Gibbs Ensemble Monte Carlo Simulations," *AIChE J.*, **43**, 1194 (1997).

Clague, D. S., and R. J. Phillips, "Hindered Diffusion of Spherical Macromolecules Through Dilute Fibrous Media," *Phys. Fluids*, **8**, 1720 (1996).

Cooper, E. R., and G. Kasting, "Transport across Epithelial Membranes," *J. Controlled Release*, **6**, 23 (1987).

Edelhauser, H. F., R. A. Hyndiuk, A. Zeeb, and R. O. Schultz, "Corneal Edema and the Intraocular Use of Epinephrine," *Amer. J. Ophthalmol.*, **93**, 327 (1982).

Ethier, C. R., "Hydrodynamics of Flow Through Gels: Application to the Eye," SM Thesis, Dept. of Chemical Engineering, Massachusetts Institute of Technology, Cambridge, (1983).

Fatt, I., and B. O. Hedbys, "Flow Conductivity of Human Corneal Stroma," *Exp. Eye Res.*, **10**, 237 (1970a).

Fatt, I., and B. O. Hedbys, "Flow of Water in the Sclera," *Exp. Eye Res.*, **10**, 243 (1970b).

Fatt, I., and B. A. Weissman, *Physiology of the Eye. An Introduction to the Vegetative Functions*, 2nd ed., Butterworth-Heinemann, Boston (1992).

Foster, C. S., and M. Sainz de la Maza, *The Sclera*, Springer-Verlag, New York (1994).

Grass, G. M., and J. R. Robinson, "Mechanisms of Corneal Drug Penetration. II. Ultrastructural Analysis of Potential Pathways for Drug Movement," *J. Pharm. Sci.*, **77**, 15 (1988).

Grass, G. M., E. R. Cooper, and J. R. Robinson, "Mechanisms of Corneal Drug Penetration. III. Modeling of Molecular Transport," *J. Pharm. Sci.*, **77**, 24 (1988).

Hassel, J. R., D. A. Newsome, and V. C. Hascall, "Characterization and Biosynthesis of Proteoglycans of Corneal Stroma from Rhesus Monkey," *J. Biol. Chem.*, **254**, 12346 (1979).

Heinegård, D., and M. Paulsson," Structure and Metabolism of Proteoglycans," *Extracellular Matrix Biochemistry*, K. A. Piez, and A. H. Reddi, eds., Elsevier, New York (1984).

Higdon, J. J. L., and G. D. Ford, "Permeability of Three-Dimensional Models of Fibrous Porous Media," *J. Fluid Mech.*, **308**, 341 (1996).

Hsieh, D. S., *Drug Permeation Enhancement*, Dekker, New York (1994).

Itoi, M., "Physico-Chemical Properties of Insoluble Corneal Collagen," *Exp. Eye Res.*, **1**, 92 (1961).

Jackson, G. W. and D. F. James, "The Permeability of Fibrous Porous Media," *Can. J. Chem. Eng.*, **64**, 364 (1986).

Johansson, L., and J.-E. Löfroth, "Diffusion and Interaction in Gels and Solutions, 4. Hard Sphere Brownian Dynamics Simulations," *J. Chem. Phys.*, **98**, 7471 (1993).

Johnson, E. M., D. A. Berk, R. K. Jain, and W. M. Deen, "Diffusion and Partitioning of Proteins in Charged Agarose Gels," *Biophys. J.*, **68**, 1561 (1995).

Johnson, E. M., D. A. Berk, R. K. Jain, and W. M. Deen, "Hindered Diffusion in Agarose Gels: Test of Effective Medium Model," *Biophys. J.*, **70**, 1017 (1996).

Johnson, E. M., and W. M. Deen, "Electrostatic Effects on the Equilibrium Partitioning of Spherical Colloids in Random Fibrous Media," *J. Colloid Interface Sci.*, **17**, 749 (1996).

Klintworth, G. K., "Macular Corneal Dystrophy: A Localized Disorder of Mucopolysaccharide Metabolism?" *Clinical, Structural, and Biochemical Advances in Hereditary Eye Disorders*, D. Daentl, ed., Liss, New York (1982).

Lang, J. C., "Ocular Drug Delivery: Conventional Ocular Formulations," *Adv. Drug Delivery Rev.*, **16**, 39 (1995).

Laurent, T. C., and J. Killander, "A Theory of Gel Filtration and Its Experimental Verification," *J. Chromatograph.*, **14**, 317 (1964).

Lehninger, A. L., D. L. Nelson, and M. M. Cox, *Principles of Biochemistry*, 2nd ed., Worth, New York (1993).

Liaw, J., and J. R. Robinson, "Ocular Penetration Enhancers," *Ophthalmic Drug Delivery Systems*, A. K. Mitra, ed., Dekker, New York (1993).

Maurice, D. M., and J. Polgar, "Diffusion Across the Sclera," *Exp. Eye Res.*, **25**, 577 (1977).

Meek, K. M., and D. W. Leonard, "Ultrastructure of Corneal Stroma: A Comparative Study," *Biophys. J.*, **64**, 273 (1993).

Ogston, A. G., "The Spaces in a Uniform Random Suspension of Fibres," *Trans. Faraday Soc.*, **54**, 1754 (1958).

Ogston, A. G., B. N. Preston, and J. D. Wells, "On the Transport of Compact Particles Through Solutions of Chain-Polymers," *Proc. R. Soc. Lond.* A, **33**, 297 (1973).

Olsen, T. W., H. F. Edelhauser, J. L. Lim, and D. H. Geroski, "Human Scleral Permeability: Effects of Age, Cryotherapy, Transscleral Diode Laser, and Surgical Thinning," *Invest. Ophthalmol. Visual Sci.*, **36**, 1893 (1995).

Panwar, Y., and J. L. Anderson, "Hindered Diffusion in Slit Pores: An Analytical Result," *Ind. Eng. Chem. Res.*, **32**, 743 (1993).

Perrins, W. T., D. R. McKenzie, and R. C. McPhedran, "Transport Properties of Regular Arrays of Cylinders," *Proc. R. Soc. Lond. A*, **369**, 207 (1979).

Prausnitz, M. R., and J. Noonan, Personal Communication, in preparation, (1997).
Reid, R. C., J. M. Prausnitz, and T. K. Sherwood, *The Properties of Gases and Liquids*, 4th ed., McGraw-Hill, New York (1987).
Robinson, J. R., and V. H. Lee, *Controlled Drug Delivery: Fundamentals and Applications*, 2nd ed., Dekker, New York (1988).
Schoenwald, R. D., "The Control of Drug Bioavailability from Ophthalmic Dosage Forms," *Controlled Drug Bioavailability: Bioavailability Control by Drug Delivery System Design*, V. F. Smolen, and L. Ball, eds., J. Wiley, New York (1985).
Tanford, C., S. A. Swanson, and W. S. Shore, "Hydrogen Ion Equilibria of Bovine Serum Albumin," *J. Amer. Chem. Soc.*, **77**, 6414 (1955).
Tasman, W., ed., *Duane's Foundations of Clinical Ophthalmology*, Lippincott-Raven, Philadelphia (1995).
Vilker, V. L., C. K. Colton, and K. A. Smith, "The Osmotic Pressure of Concentrated Protein Solutions: Effect of Concentration and pH in Saline Solutions of Bovine Serum Albumin," *J. Colloid Interface Sci.*, **79**, 548 (1981).
Weast, R. C., ed., *Handbook of Chemistry and Physics*, 77th ed., CRC Press, Cleveland (1996).
Yoshida, F., and J. G. Topliss, "Unified Model for the Corneal Permeability of Related and Diverse Compounds with Respect to their Physicochemical Properties," *J. Pharm. Sci.*, **85**, 819 (1996).

Appendix: Calculation of the Boltzmann Factor

The parameters needed to determine the Boltzmann factor in Eq. 10 are the surface-charge density of the solute, that of the fibers, and the Debye length. The Debye length was determined as 0.76 nm, based upon the composition of the BBS Plus buffer used in most studies (Alcon Surgical, 1991).

An estimate of the surface-charge density of GAG fibers in the stroma was obtained as follows. Keratan sulfate (KS) proteoglycans account for 45–60% of the total sulfated glycosaminoglycans in the stroma (Klintworth, 1982). Each KS chain consists of 30 to 50 repeat disaccharide units (Heinegård and Paulsson, 1984), with one charge group per unit (1.6×10^{-19} C per charge), yielding $\sim 40\cdot(1.6\times 10^{-19}) = 6.4\times 10^{-18}$ C per KS chain. The radius of the proteoglycan monomer, which corresponds to chain length, has been estimated as 12 nm (Axelsson and Heinegård, 1978). The GAG radius was taken as 0.5 nm in this study, resulting in a chain surface area of $2\pi\cdot(12)\cdot(0.5) = 37.7$ nm^2. The surface-charge density of the GAGs is thus estimated as 0.17 C/m^2.

For lack of necessary data, the surface charge of GAG-associated protein fibers was estimated as 0.17 C/m^2, assuming that the average surface-charge density is that of the GAGs. Although the average protein fiber charge is less than the charge on each KS chain, the average fiber surface area is also less than that of each chain, which suggests that this estimate may be reasonable.

Determination of the fiber-charge density in the sclera also required simplifying assumptions. The sclera contains mostly dermatan sulfate (DS) proteoglycans; however, the structure of the DS chains is extremely variable in the tissue itself (Heinegård and Paulsson, 1984). We therefore did not attempt to estimate the surface-charge density of the chains, and assumed instead that the fiber surface-charge density was the same in stroma and sclera.

The surface-charge density of solutes was determined from literature data. Solute surface area was determined using solute radii shown in Tables 2–5 and assuming spherical shape. The charge of small solutes was determined from solute pKa and the experimental pH (Prausnitz and Noonan, 1997). The charge number of BSA at pH = 7.4 was taken as -20.4 (Vilker et al., 1981). The charge of RISA should be approximately the same as BSA (Tanford et al., 1955). Lacking necessary information about the charge number of hemoglobin and IgG at pH = 7.4, we performed calculations assuming values of either -10 or -20.

Manuscript received Apr. 24, 1997, and revision received Sept. 22, 1997.